Talanta 297 (2026) 128692

Contents lists available at ScienceDirect

Talanta

journal homepage: www.elsevier.com/locate/talanta

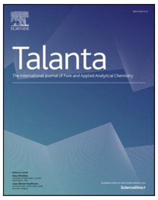

3D-printed SPME-based wooden-tip mass spectrometry for rapid detection of organic ultraviolet absorbers in complex matrices

Yingyuan Zhang [a,b,1], Deshuo Gao [a,1], Kefu Yu [a], Ruijie Zhang [a], Jiayu Zhang [a], Wenfeng Yu [a], Shiguo Chen [b], Jiying Pei [a,*]

[a] *Guangxi Laboratory on the Study of Coral Reefs in the South China Sea, Coral Reef Research Center of China, School of Marine Sciences, Guangxi University, Nanning, 530004, China*

[b] *School of Resources, Environment and Materials, Guangxi University, Nanning, 530004, China*

ARTICLE INFO

Keywords:
Wooden-tip ambient mass spectrometry
Solid-phase microextraction
3D printing
Organic ultraviolet absorber
Complex matrix

ABSTRACT

Organic ultraviolet absorbers (OUVs), commonly used in sunscreens and industrial products, have raised growing environmental and health concerns due to their pervasive occurrence in aquatic ecosystems. Conventional analytical techniques, such as liquid chromatography-mass spectrometry (LC-MS) and gas chromatography-mass spectrometry (GC-MS), offer high sensitivity but are constrained by labor-intensive workflows and extensive solvent use. Here, we present a rapid and portable screening method for seven priority OUVs by integrating a C_{18}-modified wooden-tip solid-phase microextraction (SPME) probe with ambient mass spectrometry (AMS). A custom-designed 3D-printed interface was designed to precisely align the ionization source with the mass spectrometer, enhancing stability, reproducibility, and operational ease. Detection limits (LODs) ranged from 0.23 μg/L to 8.17 μg/L, sufficient for high-exposure scenarios such as recreational waters (up to μg/L level) and the permitted concentration range in personal care products (typically 2–10 %, *w/w*). While the sensitivity is lower than that of LC-MS or GC-MS, the method achieves comparable extraction recoveries (81.3–119.6 %) in ultrapure water and post-cleansing facial rinses. In artificial seawater, recoveries dropped to 50.9–83.0 % due to salt and organic matter interfering with ionization. Despite this, the total analysis time was significantly reduced-from hours to minutes-without complex sample preparation. Field applications demonstrate the method's practicality: (1) OUVs in commercial sunscreens matched labeled ingredients; (2) surfactant-assisted cleansing increased OUV release from the skin by 1.58–2.31 times compared to water rinsing; and (3) benzophenone-1 (BP-1), 2-ethylhexyl-4-methoxycinnamate (EHMC), and ethylhexyl dimethyl *p*-aminobenzoic acid (ODPABA) were detected in swimming pool and coral reef waters, with concentrations up to 55.59 μg/L. This study provides an efficient, low-cost, and environmentally friendly alternative for rapid OUV screening and environmental risk assessment.

1. Introduction

Organic ultraviolet absorbers (OUVs) are synthetic compounds widely incorporated into sunscreens, cosmetics, and plastic products to shield against harmful ultraviolet (UV) radiation [1]. While they effectively prevent UV-induced skin damage and material degradation, their extensive use has raised growing environmental and human health concerns. OUVs are commonly released into aquatic environments through wastewater discharge and recreational activities, eventually reaching marine ecosystems [2]. Accumulating evidence suggests that these compounds can exert toxic effects on marine life, including coral bleaching [3], increased mortality in clownfish [4], and inhibited development in sea urchins [5]. Moreover, certain OUVs have been identified as potential endocrine disruptors, raising concerns about their long-term health impacts in humans [6]. Given their environmental persistence, ecological risks, and widespread use, there is an urgent demand for fast, high-throughput, and portable analytical platforms to support both environmental monitoring and industrial quality control. In coral reef ecosystems, where compounds such as benzophenone-3 (BP-3), 2-ethylhexyl-4-methoxycinnamate (EHMC), and

---

* Corresponding author.
E-mail address: pjying@gxu.edu.cn (J. Pei).

[1] The authors contributed equally to this work.

https://doi.org/10.1016/j.talanta.2025.128692
Received 28 May 2025; Received in revised form 15 July 2025; Accepted 7 August 2025
Available online 8 August 2025
0039-9140/© 2025 Elsevier B.V. All rights are reserved, including those for text and data mining, AI training, and similar technologies.

4-methylbenzylidene camphor (4-MBC) are banned in regions like Hawaii, Palau, and the U.S. Virgin Islands [7], OUV concentrations as high as 200 μg/L have still been reported in nearby waters [8]. This underscores the need for rapid, on-site screening of tourist sunscreens at entry points to help prevent further reef contamination. Similarly, in the personal care industry, fast quantification of OUVs is vital for improving analytical throughput, enabling routine product safety assessments, and ensuring compliance with regulatory limits that generally cap concentrations at 10 % (*w*/*w*) in cosmetic products [9].

Traditional chromatographic-mass spectrometric techniques, such as gas chromatography-mass spectrometry (GC-MS) [10] and liquid chromatography-mass spectrometry (LC-MS) [11], offer excellent sensitivity for detecting OUVs. Their detection limits (LODs) often reach ppt to ppb levels (Table 1) [12]. However, these methods are fundamentally limited by their reliance on labor-intensive and time-consuming workflows. This is primarily due to mandatory sample preparation procedures, such as solid-phase extraction (SPE) and liquid-liquid extraction (LLE) [13]. Sample preparation and chromatographic runs typically require tens of minutes to several hours per sample. In addition, large volumes of organic solvents (for LC) or carrier gases (for GC) are consumed, which increases environmental burden and operational complexity. These factors, along with the high cost of consumables like SPE cartridges and chromatographic columns, limit their practicality for high-throughput or on-site analysis.

To address these limitations, ambient mass spectrometry (AMS) has emerged as a promising alternative [14]. Techniques such as paper spray, wooden-tip (WT), and coated blade spray (CBS) enable direct analysis of complex samples with minimal or no pretreatment. For instance, low-temperature plasma ionization mass spectrometry (LTP-MS) has shown promise for the semi-quantitative screening of OUVs in personal care products [15]. Among AMS methods, the WT approach offers clear advantages for field environmental analysis. Unlike chromatographic paper, which can deform and affect spray stability and ionization [16], wooden tips provide greater mechanical strength and stability. Compared to CBS with sharp metal blades that pose handling risks [17], wooden tips are safer and easier to use on-site. Additionally, wood's hydroxyl-rich surface allows easy chemical modification without the oxide removal steps needed for metal substrates [18]. Despite these benefits, AMS is often limited by poor sensitivity, low reproducibility, and compromised quantitative accuracy [19] caused by matrix effects like ion suppression. Without sample cleanup, salts and other interferents compete with analytes during ionization, reducing signal strength.

To overcome this, solid-phase microextraction (SPME) is widely integrated with AMS [20]. SPME selectively captures and enriches target compounds while removing matrix interferences, offering both preconcentration and cleanup. This coupling substantially mitigates matrix effects, thereby improving ionization efficiency, enhancing sensitivity, and increasing quantitative reliability in AMS-based analyses. Recent developments such as CBS probes demonstrate the feasibility of SPME-AMS for detecting pharmaceuticals in complex biological samples [21]. Nevertheless, broader adoption of SPME-AMS is hindered by lack of standardized platforms and the need for manual probe alignment, which causes variability. Recent advances in 3D printing offer a solution by enabling the fabrication of modular, reproducible components tailored for AMS application [22]. For example, integration of 3D-printed interfaces in CBS-MS has enhanced portability and consistency in clinical analyses [23]. Therefore, combining 3D-printed modules with wooden-tip ambient mass spectrometry (WT-AMS) has great potential to enhance robustness, stability, and usability for OUV detection.

Table 1

Summary of analytical performance of conventional OUV detection methods.

Methods	Category	Analysis time (min)	Solvent-free	Cost	On-site or LOD
Preparation	SPE	10–60	×	Tens $/col.	Limited
	LLE	10–60	× (high use)	Low-medium	Limited
Detection	GC-MS	10–30	√ (but need carrier gas)	Hundreds $/col.	ppt-ppb
	LC-MS	10–30	× (as mobile phase)	Hundreds $/col.	ppt-ppb

Note: "col." stands for column.

In this study, we present the first integration of 3D-printed SPME-based WT-AMS for the rapid detection of seven high-priority OUVs in complex samples including sunscreen and water matrices. These target compounds are benzophenone-1 (BP-1), BP-3, benzophenone-8 (BP-8), EHMC, avobenzone (AVO), 4-MBC, and ethylhexyl dimethyl *p*-aminobenzoic acid (ODPABA). These target compounds were selected based on their widespread use in commercial sunscreen formulations [24] and their frequent detection in aquatic environments, where they pose potential risks to human and ecological health. Our approach combines: (1) the simplicity and high-throughput of WT-AMS, (2) the selectivity of functionalized SPME coatings, and (3) the precision and reproducibility afforded by 3D-printed interfaces. Application to real-world samples demonstrates its potential as a portable, efficient tool for environmental monitoring and industrial quality control of OUVs.

2. Experimental

2.1. Chemicals and materials

Dimethyloctadecyl[3-(trimethoxysilyl)propyl]ammonium chloride (DMOAP, C_{18} for SPME modification, 60 % in methanol) and anhydrous *N,N*-dimethylformamide (DMF, 99.8 %) were supplied by J&K Scientific Ltd. (Beijing, China). OUVs, including BP-1, BP-3, BP-8, AVO (>99 %), ODPABA (>98 %), and EHMC (>96 %), were obtained from TCI Chemicals (Shanghai, China). Additionally, 4-MBC (>99 %) was sourced from AccuStandard (USA). The isotopically labeled internal standard (IS), oxybenzone-d5 (BP-3-d5), was purchased from Sigma-Aldrich (St. Louis, USA). LC-MS grade methanol and acetonitrile were purchased from CNW Technologies (Germany). Ultrapure water (18.2 MΩ·cm) was produced using a Milli-Q purification system (Millipore, Bedford, USA).

Wooden toothpicks were purchased locally from a supermarket. Eight sunscreen products were acquired via Taobao (Alibaba Group, China). The 3D-printed SPME assembly including an immobilization station (using polylactic acid (PLA) filament from SUNLU, Zhuhai, China) and an aluminum alloy probe holder (using AlSi10Mg aluminum alloy powder, Dongguan, China), were fabricated with a Bambu Lab A1 mini 3D printer (Shenzhen, China) and a ZRapid Tech AFS420 metal 3D printer (Suzhou, China). Copper sheets for electrical connections were sourced locally.

2.2. Pretreatment of toothpick

The wooden toothpick tips were sharpened to a final diameter of 0.15–0.2 mm and trimmed to ~3 cm in length using a precision cutter. The sharpened tips were ultrasonically cleaned in methanol and air-dried. Surface modification was performed following Deng's protocol [25]: dried tips were dispersed in 40 mL of anhydrous DMF, followed by addition of 2 mL of DMOAP under vigorous stirring. The mixture was refluxed at 120 °C for 12 h under nitrogen to facilitate silanization. Post-reaction, the modified tips were rinsed with methanol and dried. In our current protocol, approximately 40 C_{18}-modified probes are prepared in parallel per batch. This number can be further increased by scaling up the volume of the reaction vessel. Due to their low cost and suitability for large-scale production, the SPME probes were designed for single use, eliminating the need for reuse and thereby reducing the risk of cross-contamination and variability in analytical performance.

2.3. Optimization of SPME extraction conditions and application to real samples

Stirring time and stirring speed are key parameters affecting SPME performance. Preliminary experiments were conducted to define suitable optimization ranges. Tests at 0, 30, 60, and 90 min showed that the signal decreased significantly at 60 min (Fig. S1), likely due to the establishment of a dynamic adsorption-desorption equilibrium. Therefore, the extraction time was further optimized within 0–50 min. Similarly, stirring speeds above 800 rpm led to bubble formation on the probe, forming a gas-film barrier that reduced extraction efficiency [26]. Based on this, the stirring speed was optimized within the range of 0–800 rpm.

Seawater samples were collected from two coral reef sites in Semporna, Malaysia: Timba Timba Island (4.548893°N, 118.929445°E) and Mataking Island (4.597790°N, 118.949882°E). A total of 500 mL of seawater was collected at each site and immediately filtered onboard using 4.5 μm membrane filters. After filtration, the samples were stored under refrigerated conditions until further processing in the laboratory. Swimming pool water was sampled from an outdoor pool with high swimmer activity on a Sunday and promptly transported to the laboratory for analysis. For extraction, 4 mL aliquots of seawater were enriched using C_{18}-modified probes by direct immersion under optimized conditions (30 min at 500 rpm with constant stirring). After extraction, the probes were rinsed with ultrapure water to eliminate residual matrix components prior to mass spectrometry (MS) analysis.

For sunscreen samples, approximately 0.1 g of product was mixed with 10 mL of methanol in a 15 mL glass vial and vortexed for 30 s to ensure complete homogenization. OUVs were extracted by ultrasonication, and a 5 mL portion of this extract was then diluted to 50 mL with ultrapure water and subjected to the same SPME procedure as described for seawater samples.

2.4. Mass spectrometry analysis

The C_{18}-modified probe, containing enriched OUVs, was secured in its holder and mounted onto the custom 3D-printed immobilization station for MS analysis. For each measurement, 20 μL of solvent was applied to the modified tip and allowed to equilibrate for 5 s to promote effective desorption of target analytes. Ionization was subsequently initiated by introducing an additional 30 μL of solvent under high-voltage conditions. To maximize signal intensity, key experimental parameters were systematically optimized. These included the orientation of the wooden tip relative to the MS ion transfer inlet, the applied spray voltage, the distance between the tip and the MS inlet, and the composition of the spray solvent. The tested ranges were selected based on previous studies and preliminary tests. Spray voltage (3.5–5 kV) was chosen because lower voltages could not sustain stable spray, while higher voltages caused discharge [27]. The tip-to-inlet distance (0.1–1 cm) was selected to optimize ion transmission while preventing electrical discharge and contamination of the MS inlet [28]. Spray angles (0°, 45°, 90°) represent common geometries in similar ambient ionization setups [29]. Solvent mixtures (methanol-acetonitrile from 1:0 to 0:1) were tested to cover different polarities and optimize desorption and ionization efficiency.

All experiments were performed using an LTQ mass spectrometer (Thermo Scientific, San Jose, USA). Mass spectra were acquired in positive ion mode with the inlet temperature set at 275 °C. Tandem mass spectrometry (MS/MS) was performed using helium as the collision gas, with collision-induced dissociation (CID) energy set at 35–50 %, an activation time of 30 ms, and an isolation width of m/z 1.0. All other instrument parameters were kept at their default settings.

2.5. Quality control

To ensure analytical reliability and minimize contamination risks, a comprehensive quality assurance and quality control (QA/QC) protocol was implemented throughout the sample collection and analysis processes. Procedural blanks were analyzed to verify the absence of contamination and matrix interference. Artificial seawater was employed as the blank matrix for marine samples, while commercial sunscreens containing only inorganic UV filters (titanium dioxide and zinc oxide) without any OUVs served as cosmetic blanks. None of the seven target OUVs were detected in these blanks, confirming negligible background contamination from reagents or materials.

To minimize contamination during field sampling, plastic containers were generally avoided due to the potential presence of residual OUVs. Swimming pool water samples were collected using amber glass bottles. For seawater samples, pre-cleaned polypropylene containers were used in the field for practical reasons, but potential contamination was evaluated by comparison with ultrapure water blanks and confirmed to be negligible. Field operators also avoided applying sunscreen or other personal care products prior to sampling.

Each matrix was spiked with known concentrations of the target OUVs, and recovery was evaluated by comparing the signal responses from spiked blank extracts to the corresponding nominal spike levels. Notably, glucose was added to the artificial seawater (35 ‰) at a concentration of 6.25 mg/L to better simulate real-world marine conditions. This corresponds to approximately 2.5 mg C/L of DOC, a level commonly observed in nearshore coastal waters [30], to mimic natural organic matter presence.

LODs and limits of quantitation (LOQs) were calculated using the standard deviation of eleven replicate blank measurements and the calibration curve slope. Specifically, LODs were defined as three times the standard deviation (3σ) divided by the calibration slope, while LOQs were defined as ten times the standard deviation (10σ) divided by the slope [31].

3. Result and discussion

3.1. 3D-printed assembly for SPME-based WT-AMS ionization

To ensure stable ionization and improve operational reproducibility in WT-AMS, we developed a 3D-printed assembly consisting of two modular components: a fixed base and a detachable metal holder (Fig. 1). This design aims to ensure precise spatial alignment and stable electrical contact between the SPME wooden tip and the MS inlet. The metal holder features a precision-drilled aperture that securely accommodates disposable wooden toothpicks used as SPME probes. A copper sheet is embedded at the interface between the holder and the base to facilitate reliable high-voltage transmission, ensuring consistent spray ionization during analysis. This modular configuration offers two key advantages. First, it maintains fixed spatial alignment between the probe and MS inlet, improving ionization consistency. Second, it ensures reliable electrical contact. Importantly, by isolating the replaceable holder from the fixed alignment structure, the design eliminates the need for realignment during probe replacement, which is a common issue in custom AMS systems [32].

The assembly demonstrated excellent mechanical robustness, showing no structural deformation after more than one year of repeated use. This durability stems from the minimal mechanical load during operation since the main function is simply to hold the wooden tip while the copper sheet serves as the electrode. Although PLA is known to be sensitive to organic solvents [33], this concern is mitigated in our design. The spray solvent is applied at the wooden tip, which is physically isolated from the PLA base by the metal holder and copper sheet. As a result, solvent-induced dissolution or chemical leaching from the PLA is effectively prevented [17]. Recent developments in 3D printing of sustainable materials, such as all-natural flame-retardant hydrogels, further underscore the relevance of modular, low-cost, and environmentally friendly fabrication strategies in analytical instrumentation design [34]. Consistent with this trend, our assembly produced

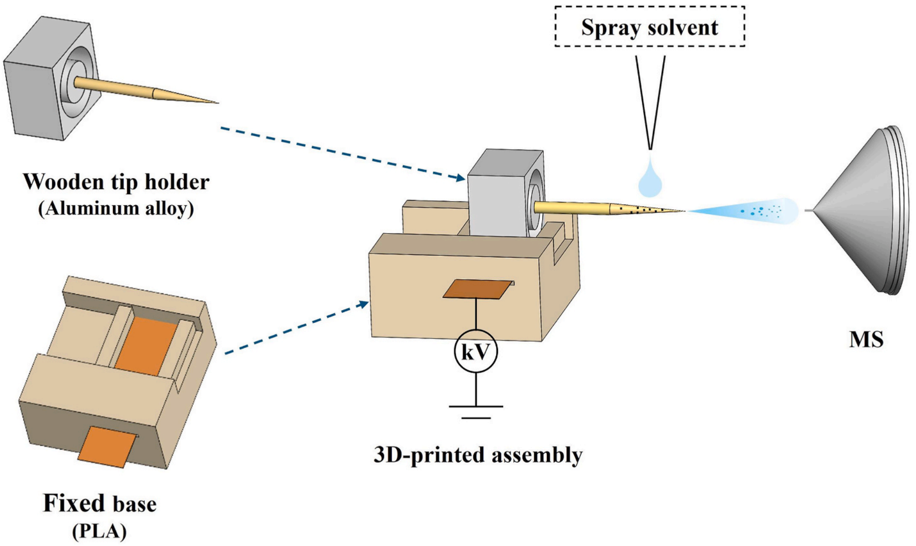

Fig. 1. Schematic diagram of the 3D-printed SPME-based WT-AMS assembly.

negligible background signals and consistent performance across repeated use. Overall, this user-friendly, low-cost, and scalable platform is well suited for laboratories developing prototype AMS systems requiring frequent probe changes.

3.2. Optimization of extraction conditions

To enhance the analytical performance of the SPME-based WT-AMS assembly, we first pretreated wooden toothpick probes with methanol prior to C_{18} surface modified. This step effectively removed surface contaminants, minimizing background noise and ion suppression during analysis [29].

As illustrated in Fig. 2a, the total ion chromatogram (TIC) obtained from the WT spray remained stable for the initial 0.6 min before gradually declining due to solvent evaporation. To ensure consistent quantification, only signal intensities within this 0.6-min window were used. For improved sensitivity and selectivity, MS/MS was employed. Characteristic fragment ions were selected based on signal strength and fragmentation specificity. As shown in Fig. 2b, the selected product ions were: *m/z* 137 for BP-1, 151 for BP-3, 121 for BP-8, 166 for ODPABA, 157 for 4-MBC, 161 for AVO, and 179 for EHMC. These ions were used for all subsequent quantification.

Given the proven efficiency of C_{18}-functionalized silica in conventional SPE [18], we evaluated the effect of C_{18} modification on our

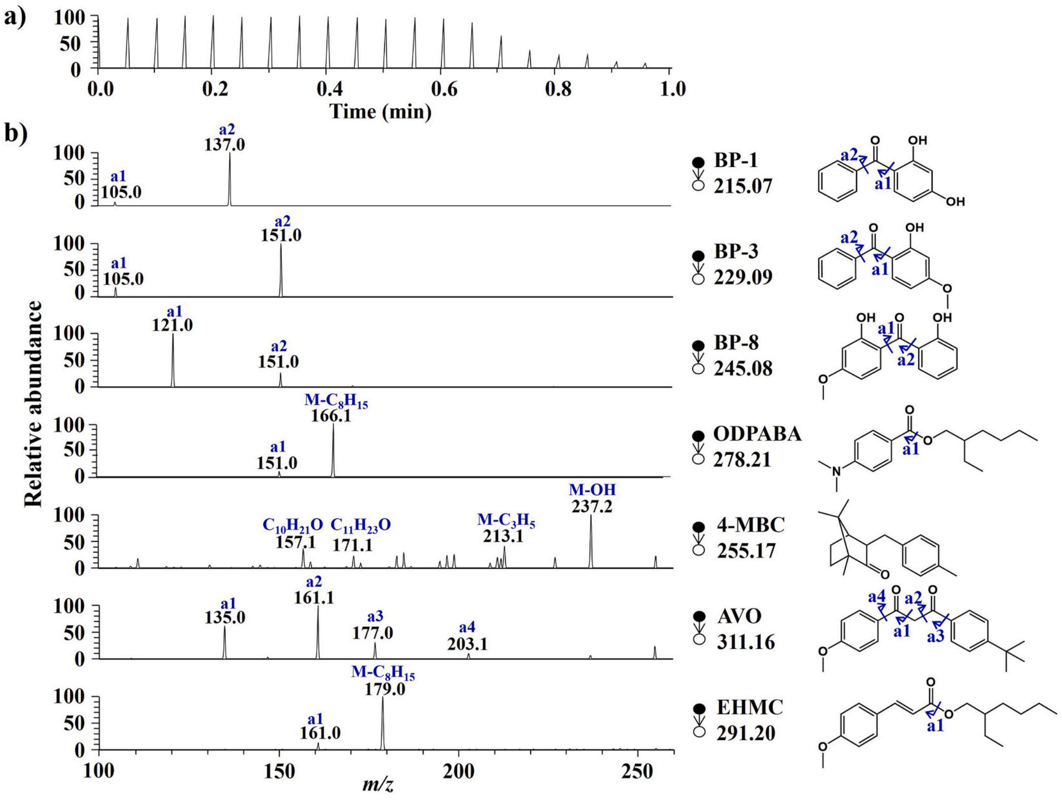

Fig. 2. a) TIC and b) MS/MS data for the seven target OUVs.

WT-AMS probes. Comparison between unmodified and C_{18}-modified wooden tips revealed significant signal enhancement across all seven analytes (Fig. 3). Enrichment factors (EFs) ranged from 2.0 for 4-MBC to 48.9 for BP-1. This variability likely reflects differences in the physicochemical properties of each compound, such as hydrophobicity, molecular weight, and steric effects [35].

Further optimization focused on extraction parameters. Extraction time and agitation speed were systematically tested. Optimal performance was achieved at 30 min extraction time and 500 rpm agitation (Fig. S2), which were applied in all subsequent experiments.

3.3. Optimization of mass spectrometry conditions

Several key parameters affecting ionization efficiency and signal quality were optimized, including the spatial orientation and distance between the wooden tip and the MS inlet, spray voltage, and spray solvent composition.

The spatial orientation of the wooden tip plays a critical role in modulating ion flow and minimizing contamination of the mass spectrometer inlet. To identify the optimal geometry, three orientations (0°, 45°, and 90° relative to the MS inlet) were tested (Fig. S3a). At 0° and 45°, mass spectra exhibited elevated background noise and poor fragmentation resolution for representative OUVs (BP-1, ODPABA, AVO, and EHMC), indicative of substantial spectral interference (Fig. S3b). In contrast, the 90° orientation yielded cleaner spectra and the highest signal intensities for all seven analytes (Fig. 4a). This improvement is likely due to the minimized entry of neutral or non-ionized species into the MS inlet, a common issue in ambient ionization techniques such as WT-AMS [29]. Therefore, the 90° configuration was adopted for all subsequent experiments.

Tip-to-inlet distance and spray voltage were further evaluated. As shown in Fig. 4b and c, optimal signal intensities for all analytes were achieved at a tip-inlet distance of 0.25 cm and a spray voltage of 4.5 kV. Distances shorter than 0.25 cm or voltages exceeding 4.5 kV led to unstable ionization due to corona discharge from localized dielectric breakdown [36,37]. Conversely, longer distances or lower voltages resulted in inefficient ion desolvation and incomplete analyte ionization, leading to diminished signal intensity [38]. Accordingly, a tip-inlet distance of 0.25 cm and a spray voltage of 4.5 kV were determined to be optimal.

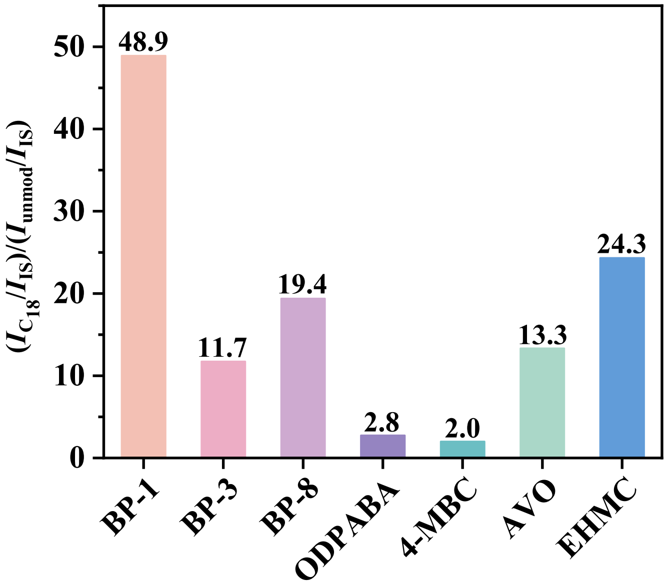

Fig. 3. EFs of seven OUVs obtained using C_{18}-modified versus unmodified SPME probes. EFs were calculated using the formula: EF = $(I_{C18}/I_{IS})/(I_{unmod}/I_{IS})$, I_{C18}/I_{IS} and I_{unmod}/I_{IS} represent the mean analyte signal intensities (n = 3) normalized to the IS for C_{18}-modified and unmodified probes, respectively.

Spray solvent composition is critical for promoting analyte desorption from the probe surface and facilitating efficient ionization. Methanol-acetonitrile mixtures were tested at varying ratios. A methanol-acetonitrile mixture of 3:7 (v/v) provided the highest signal intensities for BP-1, BP-3, BP-8, and 4-MBC, and delivered the second highest intensities for ODPABA, AVO, and EHMC (Fig. 4d). This ratio likely balances solvent polarity for efficient analyte desorption and optimal spray conditions.

3.4. Analytical performance evaluation

The analytical performance of the optimized SPME-based WT-AMS method was comprehensively evaluated in terms of reproducibility, accuracy, matrix recovery, linearity, and sensitivity. This evaluation aimed to establish the method's suitability for detecting OUVs in both environmental and cosmetic matrices.

Reproducibility is a critical parameter for AMS applications due to their susceptibility to environmental fluctuations and instrumental drift. To improve measurement stability and correct for signal variation, deuterated ISs were employed for signal normalization [19]. Following normalization, the method exhibited acceptable intermediate precision, with relative standard deviations (RSDs) ranging from 13.2 % to 23.3 % over ten replicate measurements of 0.5 mg/L samples across the seven target OUVs (Fig. S4). These values are within the acceptable range for semi-quantitative AMS methods (RSD <30 %) [39,40]. To further assess batch-to-batch consistency, we prepared three independent batches of C_{18}-modified probes, each consisting of six probes. These 18 probes were used to analyze the seven OUVs at a concentration of 0.5 mg/L. The resulting inter-batch RSDs ranged from 19.5 % to 29.9 %, demonstrating good reproducibility and minimal variability between batches (Table S1). Further improvements in reproducibility could be achieved by standardizing the WT preparation process to replace manual sharpening. Additionally, implementing an automated solvent application system would ensure more consistent solvent delivery and minimize variability caused by manual pipetting.

To evaluate potential operator bias in our SPME-based WT-AMS method, a blinded validation experiment was conducted. The operator was blinded to the true concentrations of aqueous OUV samples prepared at two levels-0 mg/L (blank) and 0.5 mg/L-with three replicates per level. As shown in Table S2, no target compounds were detected in the blank samples, confirming the absence of false positives. For the 0.5 mg/L samples, the recovery rates for the seven OUVs ranged from 94.1 % to 117.6 %, demonstrating acceptable accuracy and reliability under blinded conditions.

To assess the robustness, recovery studies were conducted using three representative media: ultrapure water, artificial seawater (simulating environmental samples) and post-cleansing facial rinse (representative of cosmetic matrices). The results showed mean recoveries ranging from 81.3 % to 119.6 % in ultrapure water and 81.4 % to 119.5 % in facial rinse (Fig. 5a). As shown in Fig. S5, the recoveries ranged from 50.9 % to 83.0 % in artificial seawater. The lower recoveries observed in artificial seawater are likely due to two contributing factors [41]: (i) the presence of dissolved organic matter, which may bind to OUVs and hinder their extraction, and (ii) high salt content, which can accumulate within the microstructures of the SPME probe and induce ion suppression during MS analysis. In comparison, both ultrapure water and facial rinse exhibited higher recoveries, suggesting minimal matrix interference and ion suppression effects in these systems. Recoveries slightly exceeding 100 % may result from pipetting variability at low volumes, matrix-induced signal enhancement [42], or trace-level background analyte residues present below the LOD in blank matrices. Despite matrix complexity, the recovery performance achieved using the WT-AMS method remains comparable to that reported for conventional SPE-based workflows [11], confirming the method's accuracy and robustness across diverse sample types.

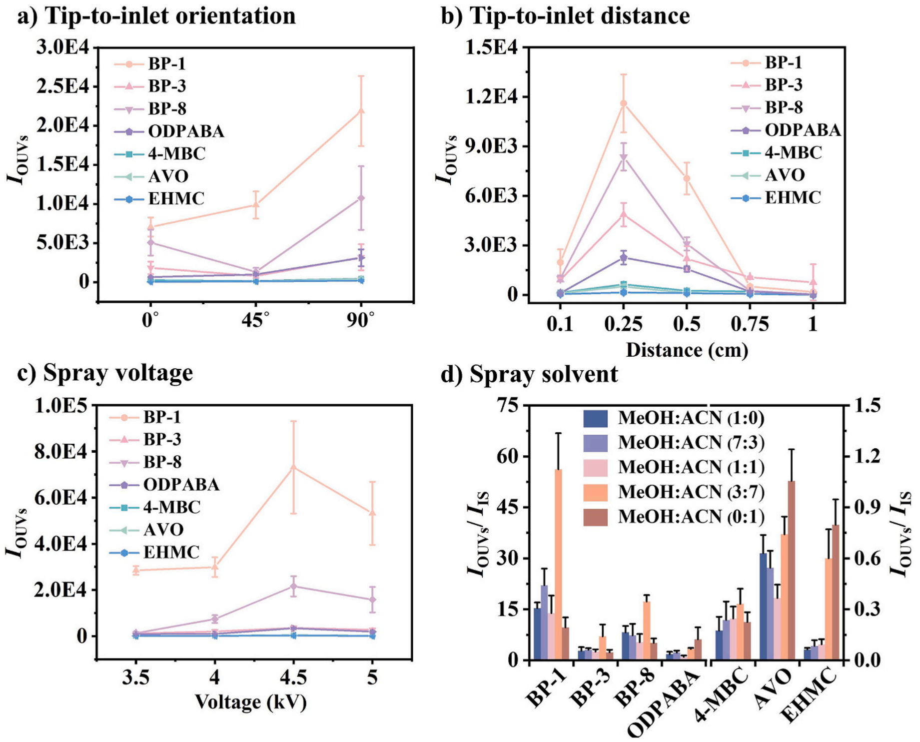

Fig. 4. Optimization of experimental parameters for the SPME-based WT-AMS method. Effect of a) tip-to-inlet orientation, b) tip-to-inlet distance, c) spray voltage, and d) spray solvent compositions on the signal intensities of the seven OUVs.

The method's quantitative capability was assessed through calibration curves constructed over a three-order-of-magnitude concentration range for each OUV (0–50 mg/L). In the 0–1 mg/L range, all analytes exhibited excellent linearity, with coefficients of determination (R^2) consistently exceeding 0.95 (Fig. 5b), indicating reliable quantification within this range. At concentrations above 1 mg/L, signal responses deviated from linearity and exhibited saturation behavior (Fig. S6), likely due to limited adsorption capacity of the SPME sorbent phase. Accordingly, the dynamic linear range for accurate quantification using this method is defined as 0–1 mg/L. The LODs were calculated to range from 0.23 μg/L to 8.17 μg/L, with corresponding LOQs between 0.78 μg/L and 27.22 μg/L. Although these LODs are higher than those typically achieved with laboratory-based LC-MS [11] or GC-MS methods [10], the trade-off is offset by significant advantages. Conventional LC-MS and GC-MS workflows require time-consuming chromatographic separation (from a few minutes to over 30 min per sample) and complex pretreatment steps such as SPE or LLE. In contrast, the SPME-based WT-AMS method provides a much simpler and faster workflow. The total analysis time is approximately 30 min per sample, primarily for the extraction step. Moreover, since extraction can be performed in parallel, the effective processing time per sample is further reduced in batch operations. By eliminating labor-intensive procedures and avoiding the use of chromatographic columns, SPE cartridges, and large volumes of organic solvents, the method not only simplifies operation but also significantly reduces costs and environmental impact. Furthermore, the portable and easy-to-assemble design enables flexible field sampling with straightforward transport back to the laboratory for analysis. Overall, the SPME-based WT-AMS method offers key advantages of speed, low cost, simplicity, and field adaptability, making it especially suitable for rapid analysis of OUVs in cosmetic and environmental samples.

3.5. Detection of real samples using our 3D-printed SPME-based WT-AMS method

To demonstrate the real-world applicability of the developed SPME-based WT-AMS method, we conducted case studies involving both commercial sunscreen products and environmental samples. These applications aim to validate the method's performance in practical scenarios and highlight its relevance for both product quality control and environmental monitoring.

Robust analytical methodologies are essential for the quality control of sunscreen products, especially given increasing regulatory restrictions on certain OUVs due to potential health risks. For example, *p*-aminobenzoic acid (PABA), a widely used UVB absorber, has been progressively banned due to its association with allergic dermatoses [43]. This highlights the need for accurate quantification of OUVs to ensure both consumer safety and regulatory compliance. To evaluate the applicability of our validated 3D-printed SPME-based WT-AMS platform, we analyzed eight commercially available sunscreen products for seven priority OUVs. As presented in Fig. 6a, EHMC, the commonly regulated UVB filter, was detected in all samples. In contrast, AVO, the broad-spectrum UVA/UVB filter, was exclusively found in Product 7. These findings aligned well with the active ingredients listed by the manufacturers. Importantly, the measured concentrations of all detected OUVs complied with current regulatory maximum allowable limits, thus confirming the platform's accuracy and suitability for product quality control and regulatory surveillance.

Beyond product composition, understanding the environmental pathways and release mechanisms of OUVs is critical, as these compounds are frequently introduced into aquatic ecosystems through domestic wastewater. A key factor influencing OUV release is consumer cleansing behavior, particularly the use of surfactant-based cleansers. Sunscreen formulations typically contain water-resistant agents such as silicones and waxes. These components make OUV residues difficult to remove by water alone [44]. Surfactants, such as sodium lauryl sulfate, facilitate the removal of these hydrophobic compounds by emulsifying

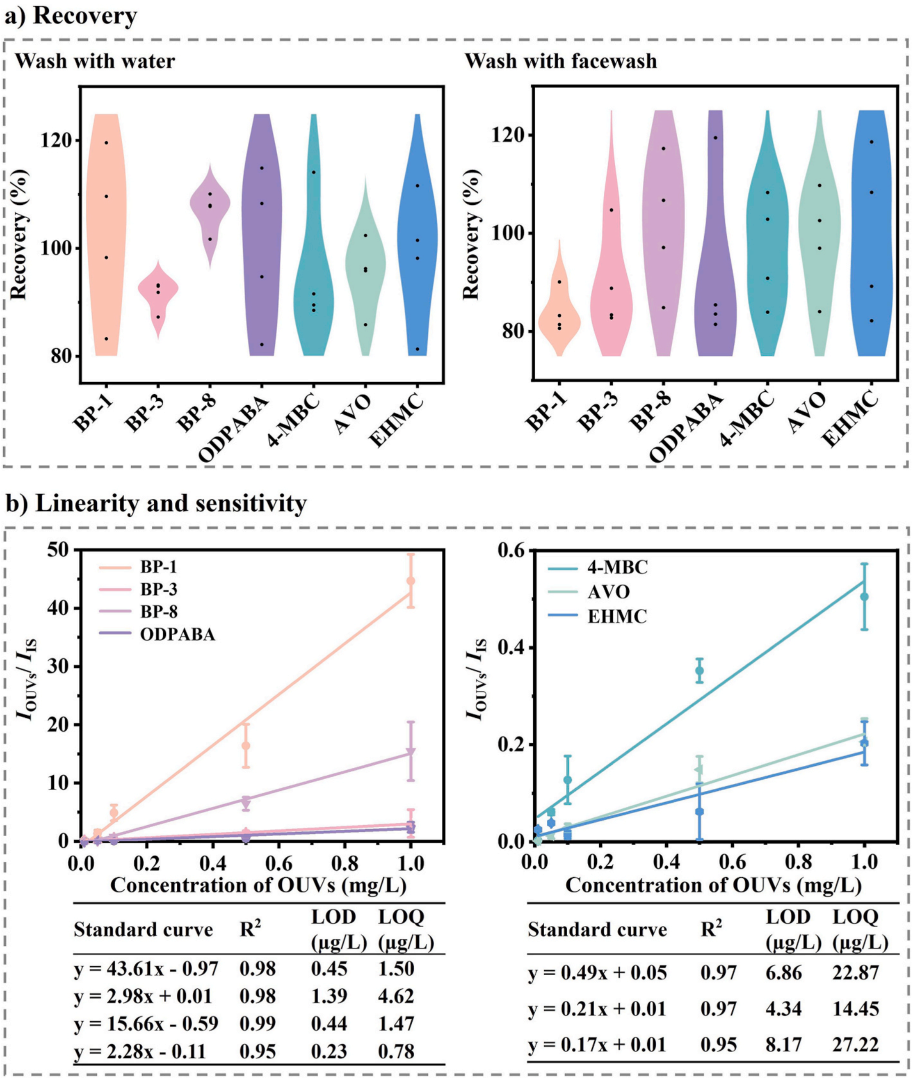

Standard curve	R^2	LOD (μg/L)	LOQ (μg/L)
y = 43.61x - 0.97	0.98	0.45	1.50
y = 2.98x + 0.01	0.98	1.39	4.62
y = 15.66x - 0.59	0.99	0.44	1.47
y = 2.28x - 0.11	0.95	0.23	0.78

Standard curve	R^2	LOD (μg/L)	LOQ (μg/L)
y = 0.49x + 0.05	0.97	6.86	22.87
y = 0.21x + 0.01	0.97	4.34	14.45
y = 0.17x + 0.01	0.95	8.17	27.22

Fig. 5. Analytical performance of the 3D-printed SPME-based WT-AMS method, including: a) recoveries across different matrices and b) linearity and sensitivity as determined from calibration curves.

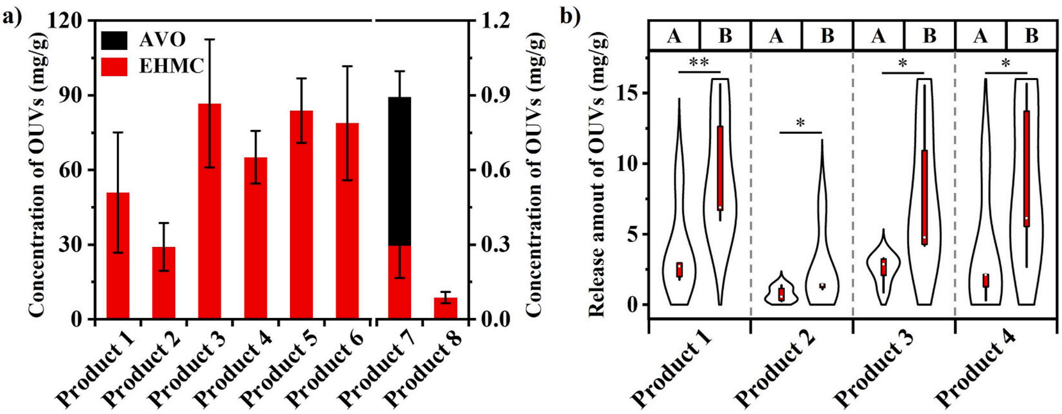

Fig. 6. a) OUV contents in eight commercially available sunscreen brands. b) Comparison of OUV release with water-only rinsing versus surfactant-assisted cleansing (**$p < 0.01$, *$p < 0.05$, ANOVA). “A” represents water-only rinsing, while “B” represents cleansing with a facial cleanser.

them. To evaluate this effect, we conducted standardized washing experiments using four representative sunscreen brands. Wastewater effluents were collected following two conditions: water-only rinsing and surfactant-assisted cleansing. As shown in Fig. 6b, surfactant use significantly increased OUV release, with concentrations 1.58 to 2.31 times higher than those from water-only rinsing ($p < 0.05$, ANOVA). These results clearly demonstrate that surfactant substantially enhance the mobilization of OUVs from the skin.

Following their release from personal care products (PCPs), OUVs are readily can be transported into aquatic environments, where they pose significant ecological and human health risks due to their potential for bioaccumulation and biomagnification [45]. In this study, both freshwater (swimming pool water) and seawater samples were analyzed to assess the presence of OUVs. In swimming pool water, BP-1 was detected at a concentration of 13.63 μg/L. Given that BP-1 is less commonly used directly in sunscreen formulations, its presence is likely attributable, at least in part, to the environmental transformation of BP-3, a widely used OUV that is known to metabolize into BP-1 [46]. Furthermore, the longer biological half-life of BP-1 relative to BP-3 indicates greater environmental persistence and a higher potential for bioaccumulation [46].

While swimming pool water represents a controlled freshwater environment with direct human input, marine ecosystems-particularly coral reefs-are more complex and vulnerable to a wider range of contaminants. To evaluate the environmental relevance of OUVs in such ecosystems, we extended our investigation to nearshore coral reef waters in Semporna, Malaysia, a region recognized as a marine biodiversity hotspot and increasingly impacted by tourism [47]. Previous studies have linked OUV contamination to adverse biological effects in corals, including bleaching, polyp retraction, impaired larval development, and increased mortality [48–50]. Seawater samples were collected from two reef sites (S1 and S2) five days after the Chinese National Day holiday (October 1–7), a period of heightened tourist activity. Analysis revealed that EHMC was present at concentrations of 25.13 μg/L at S1 and 55.59 μg/L at S2. ODPABA was also detected at 3.15 μg/L at S1 but was below the detection limit at S2. These concentrations are two to three orders of magnitude higher than typical levels reported in coastal reefs (ng/L range) and are comparable to those observed in severely impacted areas such as St. John Island, where concentrations up to 213 μg/L have been recorded [8]. In addition to OUVs released directly from recreational activities, several other sources likely contribute to the observed contamination in Semporna. Widespread plastic pollution [51,52], poor waste management [51], and weak regulatory enforcement have been reported along the coast. Degradation of vessel coatings and fishing gear may release additional OUVs, and the lack of effective wastewater treatment infrastructure leads to the discharge of untreated sewage from both coastal villages and floating settlements [53]. These findings collectively indicate a substantial anthropogenic impact on reef water quality and underscore the urgent need for coordinated monitoring and mitigation strategies to protect vulnerable marine ecosystems.

4. Conclusion

This study demonstrates the successful integration of 3D printing, SPME, and WT-AMS into a unified analytical platform for the rapid, low-cost, and environmentally friendly detection of OUVs in complex matrices. The developed method effectively overcomes key limitations of conventional chromatographic techniques-such as GC-MS and LC-MS, which typically involve costly instrumentation, labor-intensive sample pretreatment, and limited throughput. In contrast, the proposed approach offers significant advantages in operational simplicity, portability, and analytical efficiency. The optimized protocol exhibited robust analytical performance, with intermediate precision (RSD <23.3 %), satisfactory recoveries (50.9–119.6 %), and low LODs (0.23–8.17 μg/L), enabling reliable semi-quantitative analysis of seven high-priority OUVs. In addition, inter-batch RSDs of 19.5–29.9 % confirmed the method's reproducibility under varied operational conditions, while blinded recovery results between 94.1 % and 117.6 % demonstrated its accuracy and minimal operator bias. Application of the method to real-world samples provided critical insights into both product quality and environmental impact: 1) The widespread detection of regulated OUVs such as EHMC in commercial sunscreens was consistent with ingredient labels, validating the method's applicability for quality control and regulatory compliance. 2) Surfactant-assisted cleansing significantly increased OUV release into wastewater, highlighting the influence of personal hygiene practices on environmental OUV loads. 3) The detection of OUVs in real-world samples, including swimming pool water and nearshore seawater, demonstrates their environmental persistence and widespread release from PCPs. These findings underscore their potential ecological and human health risks and highlight the need for effective control and management strategies.

CRediT authorship contribution statement

Yingyuan Zhang: Writing – review & editing, Writing – original draft, Validation, Methodology, Investigation, Formal analysis, Data curation. **Deshuo Gao:** Validation, Software, Methodology, Investigation, Data curation. **Kefu Yu:** Supervision, Resources. **Ruijie Zhang:** Validation, Supervision, Resources. **Jiayu Zhang:** Validation, Investigation. **Wenfeng Yu:** Validation, Investigation. **Shiguo Chen:** Validation, Investigation. **Jiying Pei:** Writing – review & editing, Writing – original draft, Supervision, Project administration, Funding acquisition, Conceptualization.

Declaration of competing interest

The authors declare that they have no known competing financial interests or personal relationships that could have appeared to influence the work reported in this paper.

Acknowledgements

This work is supported by Guangxi Natural Science Foundation (No. 2023GXNSFAA026488), National Natural Science Foundation of China (No. 22264003), the National Innovation and Entrepreneurship Training Program for College Students (No. 202510593495).

Appendix B. Supplementary data

Supplementary data to this article can be found online at https://doi.org/10.1016/j.talanta.2025.128692.

Data availability

Data will be made available on request.

References

[1] B.R. Li, Z.Z. Yao, F. Zhao, B.Y. Meng, Z.H. Ma, C. Li, Occurrence of organic ultraviolet absorbers in the particle and gas samples from plastic greenhouses: human inhalation intake risk assessment, J. Hazard. Mater. 474 (2024) 134801, https://doi.org/10.1016/j.jhazmat.2024.134801.

[2] C.L. Mitchelmore, E.E. Burns, A. Conway, A. Heyes, I.A. Davies, A critical review of organic ultraviolet filter exposure, hazard, and risk to corals, Environ. Toxicol. Chem. 40 (2021) 967–988, https://doi.org/10.1002/etc.4948.

[3] C.M. Hansel, Sunscreens threaten coral survival, Science 376 (2022) 578–579, https://doi.org/10.1126/science.abo4627.

[4] A.N. Barone, C.E. Hayes, J.J. Kerr, R.C. Lee, D.B. Flaherty, Acute toxicity testing of TiO2-based vs. oxybenzone-based sunscreens on clownfish (Amphiprion ocellaris), Environ. Sci. Pollut. Res. 26 (2019) 14513–14520, https://doi.org/10.1007/s11356-019-04769-z.

[5] E.A. Shore, K.E. Huber, A.D. Garrett, M.H. Pespeni, Four plastic additives reduce larval growth and survival in the sea urchin Strongylocentrotus purpuratus, Mar. Pollut. Bull. 175 (2022) 113385, https://doi.org/10.1016/j.marpolbul.2022.113385.

[6] Y. Sakuragi, H. Takada, H. Sato, A. Kubota, M. Terasaki, S. Takeuchi, A. Ikeda-Araki, Y. Watanabe, S. Kitamura, H. Kojima, An analytical survey of benzotriazole UV stabilizers in plastic products and their endocrine-disrupting potential via human estrogen and androgen receptors, Sci. Total Environ. 800 (2021) 149374, https://doi.org/10.1016/j.scitotenv.2021.149374.

[7] I.B. Miller, S. Pawlowski, M.Y. Kellermann, M. Petersen-Thiery, M. Moeller, S. Nietzer, P.J. Schupp, Toxic effects of UV filters from sunscreens on coral reefs revisited: regulatory aspects for "reef safe" products, Environ. Sci. Eur. 33 (2021) 74, https://doi.org/10.1186/s12302-021-00515-w.

[8] C.A. Downs, E. Kramarsky-Winter, R. Segal, J. Fauth, S. Knutson, O. Bronstein, F. R. Ciner, R. Jeger, Y. Lichtenfeld, C.M. Woodley, P. Pennington, K. Cadenas,

A. Kushmaro, Y. Loya, Toxicopathological effects of the sunscreen UV filter, oxybenzone (benzophenone-3), on coral planulae and cultured primary cells and its environmental contamination in Hawaii and the U.S. Virgin Islands, Arch. Environ. Contam. Toxicol. 70 (2016) 265–288, https://doi.org/10.1007/s00244-015-0227-7.

[9] S.H. Mikkelsen, C. Lassen, M. Warming, E. Hansen, A. Brinch, D. Brooke, M. Crookes, E. Nielsen, J. Bredsdorff, Survey and health assessment of UV filters. Ministry of Environment and Food, DTU Food, 2015. ISBN 978-87-93352-82-7, https://i2.cdn.turner.com/cnn/2016/images/04/14/978-87-93352-82-7.pdf.

[10] K.I. Ekpeghere, U.J. Kim, O. Sung-Hee, H.Y. Kim, J.E. Oh, Distribution and seasonal occurrence of UV filters in Rivers and wastewater treatment plants in Korea, Sci. Total Environ. 542 (2016) 121–128, https://doi.org/10.1016/j.scitotenv.2015.10.033.

[11] L.N. Lyu, J. Li, Q.Y. Huang, Q. Liu, C. Yang, J.D. Dong, H.F. Su, S. Zhang, Exploring the hidden threat of organic UV filters to corals and macroalgae in coral reef ecosystem from Luhuitou, Sanya, China, Environ. Sci. Technol. 59 (2025) 8130–8139, https://doi.org/10.1021/acs.est.4c11463.

[12] S. Ramos, V. Homem, A. Alves, L. Santos, Advances in analytical methods and occurrence of organic UV-filters in the environment - a review, Sci. Total Environ. 526 (2015) 278–311, https://doi.org/10.1016/j.scitotenv.2015.04.055.

[13] J.Y. Pei, N. Liu, J.J. Hu, Y.T. Wang, K.F. Yu, R.J. Zhang, Research progress on pretreatment technique and instrumental analysis method of organic ultraviolet absorbers in environment matrices, Environmental Monitoring in China 39 (2023) 157–169, https://doi.org/10.19316/j.issn.1002-6002.2023.06.16.

[14] Z. Takáts, J.M. Wiseman, B. Gologan, R.G. Cooks, Mass spectrometry sampling under ambient conditions with desorption electrospray ionization, Science 306 (2004) 471–473, https://doi.org/10.1126/science.1104404.

[15] X. Ding, S. Gerbig, B. Spengler, S. Schulz, Reactive low temperature plasma ionization mass spectrometry for the determination of organic UV filters in personal care products, Talanta 178 (2018) 780–787, https://doi.org/10.1016/j.talanta.2017.10.021.

[16] N.E. Manicke, B.J. Bills, C.S. Zhang, Analysis of biofluids by paper spray MS: advances and challenges, Bioanalysis 8 (2016) 589–606, https://doi.org/10.4155/bio-2015-0018.

[17] W. Zhou, Q.Z. Lan, M. Dutt, J. Pawliszyn, 3D printed coated blade spray-mass spectrometry devices, Anal. Chem. 96 (2024) 16520–16524, https://doi.org/10.1021/acs.analchem.4c04613.

[18] J.W. Deng, W.Y. Li, Q.X. Yang, Y.H. Liu, L. Fang, Y.H. Guo, P.R. Guo, L. Lin, Y. Y. Yang, T.G. Luan, Biocompatible surface-coated probe for *in vivo, in situ*, and microscale lipidomics of small biological organisms and cells using mass spectrometry, Anal. Chem. 90 (2018) 6936–6944, https://doi.org/10.1021/acs.analchem.8b01218.

[19] T.H. Kuo, E.P. Dutkiewicz, J.Y. Pei, C.C. Hsu, Ambient ionization mass spectrometry today and tomorrow: embracing challenges and opportunities, Anal. Chem. 92 (2020) 2353–2363, https://doi.org/10.1021/acs.analchem.9b05454.

[20] X. Geng, Y.Q. Wang, H.L. Li, D.D.Y. Chen, Characterization of cigarette smokeomics by in situ solid-phase microextraction and confined-space direct analysis in real time mass spectrometry, Talanta 280 (2024) 126680, https://doi.org/10.1016/j.talanta.2024.126680.

[21] G.A. Gómez-Ríos, J. Pawliszyn, Development of coated blade spray ionization mass spectrometry for the quantitation of target analytes present in complex matrices, Angew. Chem. Int. Ed. 53 (2014) 14503–14507, https://doi.org/10.1002/anie.201407057.

[22] H. Guillén-Alonso, I. Rosas-Román, R. Winkler, The emerging role of 3D-printing in ion mobility spectrometry and mass spectrometry, Anal. Methods 13 (2021) 852–861, https://doi.org/10.1021/10.1039/d0ay02290j.

[23] M. Grajewski, M. Hermann, R.D. Oleschuk, E. Verpoorte, G.I. Salentijn, Leveraging 3D printing to enhance mass spectrometry: a review, Anal. Chim. Acta 1166 (2021) 338332, https://doi.org/10.1016/j.aca.2021.338332.

[24] A. Pniewska, U. Kalinowska-Lis, A survey of UV filters used in sunscreen cosmetics, Appl. Sci. 14 (2024) 3302, https://doi.org/10.3390/app14083302.

[25] J.W. Deng, Y.Y. Yang, L. Fang, L. Lin, H.Y. Zhou, T.G. Luan, Coupling solid-phase microextraction with ambient mass spectrometry using surface coated wooden-tip probe for rapid analysis of ultra trace perfluorinated compounds in complex samples, Anal. Chem. 86 (2014) 11159–11166, https://doi.org/10.1021/ac5034177.

[26] D.L. Li, H.N. Wang, L. Yang, X.K. Yan, L.J. Wang, H.J. Zhang, Intensification effects of stirred fluid on liquid–solid, gas–liquid and gas–solid interactions in flotation: a review, Chem. Eng. Process. Process Intensif. 152 (2020) 107943, https://doi.org/10.1016/j.cep.2020.107943.

[27] C. Ling, Q.F. Shi, Z.P. Wei, J.J. Zhang, J.J. Hu, J.Y. Pei, Rapid analysis of quinones in complex matrices by derivatization-based wooden-tip electrospray ionization mass spectrometry, Talanta 237 (2022) 122912, https://doi.org/10.1016/j.talanta.2021.122912.

[28] D.M. Freund, K.A. Sammons, N.P. Makunga, J.D. Cohen, A.D. Hegeman, Leaf spray mass spectrometry: a rapid ambient ionization technique to directly assess metabolites from plant tissues, J. Vis. Exp. (2018) e57949, https://doi.org/10.3791/57949.

[29] B. Hu, Z.P. Yao, Electrospray ionization mass spectrometry with wooden tips: a review, Anal. Chim. Acta 1209 (2022) 339136, https://doi.org/10.1016/j.aca.2021.339136.

[30] C. Barrón, C.M. Duarte, Dissolved organic carbon pools and export from the coastal ocean, Glob. Biogeochem. Cycles 29 (2015) 1725–1738, https://doi.org/10.1002/2014GB005056.

[31] Environmental Protection Agency, Office of science and technology, engineering and analysis division, revised assessment of detection and quantitation approaches. https://onesearch.library.northeastern.edu/permalink/01NEU_INST/fgrrp0/alma9952293931701401, 2004. (Accessed 8 July 2025).

[32] E.M. McBride, P.M. Mach, E.S. Dhummakupt, S. Dowling, D.O. Carmany, P. S. Demond, G. Rizzo, N.E. Manicke, T. Glaros, Paper spray ionization: applications and perspectives, TrAC, Trends Anal. Chem. 118 (2019) 722–730, https://doi.org/10.1016/j.trac.2019.06.028.

[33] B. Freeland, E. McCarthy, R. Balakrishnan, S. Fahy, A. Boland, K.D. Rochfort, M. Dabros, R. Marti, S.M. Kelleher, J. Gaughran, A review of polylactic acid as a replacement material for single-use laboratory components, Materials 15 (2022) 26, https://doi.org/10.3390/ma15092989.

[34] X.L. Zuo, Y. Zhou, K.G. Hao, C. Liu, R.H. Yu, A.R. Huang, C. Wu, Y.Y. Yang, 3D printed all-natural hydrogels: flame-retardant materials toward attaining green sustainability, Adv. Sci. (Weinh.) 11 (2024) e2306360, https://doi.org/10.1002/advs.202306360.

[35] P.R. Haddad, M. Taraji, R. Szücs, Prediction of analyte retention time in liquid chromatography, Anal. Chem. 93 (2021) 228–256, https://doi.org/10.1021/acs.analchem.0c04190.

[36] J.Y. Pei, C.C. Hsu, R.J. Zhang, Y.H. Wang, K.F. Yu, G.M. Huang, Unexpected reduction of iminoquinone and quinone derivatives in positive electrospray ionization mass spectrometry and possible mechanism exploration, J. Am. Soc. Mass Spectrom. 28 (2017) 2454–2461, https://doi.org/10.1007/s13361-017-1770-4.

[37] J.Y. Pei, C.C. Hsu, K.F. Yu, Y.H. Wang, G.M. Huang, Time-resolved method to distinguish protein/peptide oxidation during electrospray ionization mass spectrometry, Anal. Chim. Acta 1011 (2018) 59–67, https://doi.org/10.1016/j.aca.2018.01.025.

[38] N.B. Cech, C.G. Enke, Practical implications of some recent studies in electrospray ionization fundamentals, Mass Spectrom. Rev. 20 (2001) 362–387, https://doi.org/10.1002/mas.10008.

[39] A. Albert, J.T. Shelley, C. Engelhard, Plasma-based ambient desorption/ionization mass spectrometry: state-of-the-art in qualitative and quantitative analysis, Anal. Bioanal. Chem. 406 (2014) 6111–6127, https://doi.org/10.1007/s00216-014-7989-z.

[40] S. Gerbig, G. Stern, H.E. Brunn, R.A. Düring, B. Spengler, S. Schulz, Method development towards qualitative and semi-quantitative analysis of multiple pesticides from food surfaces and extracts by desorption electrospray ionization mass spectrometry as a preselective tool for food control, Anal. Bioanal. Chem. 409 (2017) 2107–2117, https://doi.org/10.1007/s00216-016-0157-x.

[41] J.M. Wu, X.Q. Qian, Z.G. Yang, L.F. Zhang, Study on the matrix effect in the determination of selected pharmaceutical residues in seawater by solid-phase extraction and ultra-high-performance liquid chromatography–electrospray ionization low-energy collision-induced dissociation tandem mass spectrometry, J. Chromatogr. A 1217 (2010) 1471–1475, https://doi.org/10.1016/j.chroma.2009.12.074.

[42] H. Trufelli, P. Palma, G. Famiglini, A. Cappiello, An overview of matrix effects in liquid chromatography–mass spectrometry, Mass Spectrom. Rev. 30 (2011) 491–509, https://doi.org/10.1002/mas.20298.

[43] A.J. Waters, D.R. Sandhu, G. Lowe, J. Fergson, Photocontact allergy to PABA in sunscreens: the need for continued vigilance, Contact Dermat. 60 (2009), https://doi.org/10.1111/j.1600-0536.2008.01448.x, 173-173.

[44] P.P. Agin, Water resistance and extended wear sunscreens, Dermatol. Clin. 24 (2006) 75–79, https://doi.org/10.1016/j.det.2005.08.002.

[45] J.J. Hu, C.G. Pan, F.J. Peng, H. Liang, Z.Z. Liu, K.F. Yu, An integrated multi-omics approach reveals octocrylene disrupts Tetradesmus obliquus growth by triggering a cascade of photosynthetic inhibition and metabolic dysregulation, J. Hazard. Mater. 495 (2025) 139072, https://doi.org/10.1016/j.jhazmat.2025.139072.

[46] S. Kim, K. Choi, Occurrences, toxicities, and ecological risks of benzophenone-3, a common component of organic sunscreen products: a mini-review, Environ. Int. 70 (2014) 143–157, https://doi.org/10.1016/j.envint.2014.05.015.

[47] Xinhuanet, Surge in Chinese tourist arrivals showcases strong people-to-people ties – Malaysian official. https://english.news.cn/20241001/c3690ba199d34b8da1095764dcd8f993/c.html, 2024. (Accessed 3 May 2025).

[48] D. Vuckovic, A.I. Tinoco, L. Ling, C. Renicke, J.R. Pringle, W.A. Mitch, Conversion of oxybenzone sunscreen to phototoxic glucoside conjugates by sea anemones and corals, Science 376 (2022) 644–648, https://doi.org/10.1126/science.abn2600.

[49] D. Stien, F. Clergeaud, A.M.S. Rodrigues, K. Lebaron, R. Pillot, P. Romans, S. Fagervold, P. Lebaron, Metabolomics reveal that octocrylene accumulates in pocillopora damicornis tissues as fatty acid conjugates and triggers coral cell mitochondrial dysfunction, Anal. Chem. 91 (2019) 990–995, https://doi.org/10.1021/acs.analchem.8b04187.

[50] J.Y. Pei, K. Pang, M.W. Wang, R.J. Zhang, K.F. Yu, Research progress on toxicological effects of organic ultraviolet absorbents on coral, Asian J. Ecotoxicol. 18 (2023) 51–67. https://link.cnki.net/urlid/11.5470.X.20221028.1458.008.

[51] P.L. Choo, S.R.M. Hashim, E. Saleh, R. Shapawi, Z. Waheed, Assessing anthropogenic impacts on coral reefs using local and expert knowledge in the Semporna Priority conservation area, Sabah, Malaysia, Aquat. Conserv. Mar. Freshw. Ecosyst. 35 (2025) e70108, https://doi.org/10.1002/aqc.70108.

[52] Daily Express (Malaysia), Losing the battle to plastic in semporna. https://www.dailyexpress.com.my/read/5174/losing-the-battle-to-plastic-in-semporna/, 2023. (Accessed 8 July 2025).

[53] UN Environment Programme, Enhancing wastewater, nutrient management and sanitation provision for marginalized coastal communities in Sabah, Malaysia. https://www.unep.org/topics/ocean-seas-and-coasts/ecosystem-degradation-pollution/wastewater/enhancing-wastewater?utm_source=chatgpt.com, 2024. (Accessed 8 July 2025).